JCTC Journal of Chemical Theory and Computation

ARTICLE

pubs.acs.org/JCTC

On the Calculation of the Dielectric Permittivity and Relaxation of Molecular Models in the Liquid Phase

Sereina Riniker, Anna-Pitschna E. Kunz, and Wilfred F. van Gunsteren*

Laboratory of Physical Chemistry, Swiss Federal Institute of Technology, ETH, 8093 Zürich, Switzerland

ABSTRACT: Methodology to compute the relative static dielectric permittivity and dielectric relaxation time of molecular liquids is reviewed and explicit formulas are given for the external field method in the case of simulations using a spherical cutoff, in which the background dielectric permittivity (ε_{cs}) can be larger than one, in combination with a Poisson−Boltzmann reaction-field approximation for long-range electrostatic interactions. The external field method is simple to implement and computationally efficient. It is particularly suitable for polarizable molecular models with zero permanent dipole moment and for coarse-grained molecular models with $\varepsilon_{cs} > 1$. The dielectric permittivities and relaxation times of water (H_2O), dimethylsulfoxide (DMSO), methanol (MeOH), and chloroform ($CHCl_3$), which range from 2 to 80 and from 5 ps to 50 ps, respectively, were calculated as an illustration.

1. INTRODUCTION

The interactions between molecules in the liquid phase, such as biomolecules in aqueous solution, are basically (i.e., at the quantum-chemical level) governed by electrostatic interactions. These manifest themselves in the form of Coulombic interactions between parts of molecules that have a nonzero net charge density, or of polarization interactions between electronically polarizable parts of molecules, or in the form of van der Waals interactions originating from mutual interactions between dipolar fluctuations of atoms. This implies that the dielectric properties of a molecular model for a given compound are of central importance when using such a model in a biomolecular simulation. For this reason, it is standard practice to compute and report the dielectric permittivity of molecular models for compounds that are used in such simulations. This property can be obtained from a simulation of the compound in the liquid phase.

Different methods are available to compute the dielectric permittivity (ε) of a molecular liquid via computer simulation, e.g., molecular dynamics (MD) simulation:[1]

(1) In the limit of low field strength, the fluctuations of the electric dipole moment $\vec{M}$ of the simulated system in an equilibrium simulation can be related to the polarization $\vec{P}$ induced in the system if an external electric field $\vec{E}^{ext}$ would be applied to it,[2] and thus to the dielectric permittivity ε. Technically, this relationship between the variance of the distribution of $\vec{M}$ and ε can be employed in different ways, using simulations in which $\vec{M}$ is unrestrained, or restrained by a biasing potential energy term, or constrained to a particular range of $\vec{M}$ values.[3]

(2) The dipole moment $\vec{M}$ that is induced by the application of an external field $\vec{E}^{ext}$ to the system can be analyzed to yield ε. The external field can be constant and homogeneous[4] or sinusoidal in space[5] in order to probe a range of $\vec{E}^{ext}$ values in one simulation. A variant of the external field method would be the coupling of the polarization of the system $\vec{P}^{syst}$ to an external polarization bath $\vec{P}^{bath}$, using a first-order weak coupling equation.[6]

When considering polarizable models for molecules that have zero permanent dipole moment, the fluctuating dipole moment methodology can obviously not be used, because no such fluctuations will occur in a simulation. Thus, an external field technique is the method of choice in such cases. Although this method seems simple to implement—just apply a homogeneous external field $\vec{E}^{ext}$ of a chosen value and calculate the polarization $\vec{P}$ induced in the system—the precise expressions relating $\vec{E}^{ext}$ to $\vec{P}$ and ε are dependent on the way the electrostatic interactions in the system are calculated, e.g., using a cutoff sphere, a minimum-image cutoff cube, a rectangular or oblique infinite lattice sum, or a spherical cutoff with continuum reaction field beyond the cutoff sphere. Since the first two schemes to calculate the electrostatic interactions induce sizable distortions of the configurational distribution of the system, only the latter two schemes are currently used in molecular simulations.

Each technique has advantages and disadvantages. Using a lattice-sum technique to compute long-range electrostatic interactions, one simulates an infinitely extended system in atomic detail, but at the cost of artificially enhancing periodic order in the system, which distorts the forces inside the system.[7−12] Using a spherical cutoff with a continuum reaction-field approximation representing the long-range electrostatic interactions, a distortive periodicity is avoided at the expense of a loss of atomic details beyond the cutoff sphere, which are modeled as an isotropic, homogeneous mean-field dielectric response.[13−15] In our view, this approximation is in regard to noncrystalline condensed-phase biomolecular systems less distortive than the imposition of artificial small-scale periodicity.

In the reaction-field approximation of the long-range electrostatic interactions, it is usually assumed that the dielectric continuum outside the cutoff sphere will react instantaneously to changes of the partial charges inside the cutoff sphere. In general, however, there will be a delay in the response caused by

Received: October 26, 2010
Published: April 15, 2011

classical Stokes and dielectric frictional effects in the surroundings, which can be modeled using a generalized Langevin equation for the reaction field.[13] We shall not consider this approximation of the long-range electrostatic forces, because the method is computationally expensive and an instantaneous treatment of the reaction-field turned out to be sufficiently accurate.

The original formulation of the dipolar reaction-field force induced by a dipole moment $\vec{M}$ inside a cutoff sphere through the surrounding dielectric continuum of permittivity ε_{rf}[14] was generalized[15] to the case of a dielectric continuum characterized by ε_{rf} and an ionic strength I represented by an inverse Debye screening length κ, leading to a so-called Poisson−Boltzmann reaction-field force, which reduces to the original dipolar one for $\kappa = 0$.

Here, we generalize the external field method to compute the static relative dielectric permittivity of a molecular model[4] to the case in which the background permittivity of the cutoff sphere (ε_{cs}) may be larger than one and the dielectric medium outside the cutoff sphere can have a nonzero ionic strength. We give expressions for the calculation of the dielectric permittivity ε from MD simulations in which a spherical truncation with $\varepsilon_{cs} \geq 1$ and a Poisson−Boltzmann continuum reaction field with $\kappa \geq 0$ outside the cutoff sphere is applied in combination with a constant homogeneous external field $\vec{E}^{ext}$. The external field method can also be used to obtain the Debye dielectric relaxation time τ_D from nonequilibrium MD simulations in which a homogeneous electric field is switched on. By performing simulations at different field strengths and measuring the polarization response, precise values of ε and τ_D can be obtained. The expressions for the static (i.e., zero frequency), relative dielectric permittivity $\varepsilon(0)$ and for the Debye relaxation time of the model, as a function of the magnitude of $\vec{E}^{ext}$, are tested via application to models of different molecular liquids (chloroform ($CHCl_3$), methanol (MeOH), dimethylsulfoxide (DMSO), and water (H_2O)) that cover a wide range of $\varepsilon(0)$ values (i.e., 2−80) and of τ_D values (i.e., 5−50 ps), and comparison to the $\varepsilon(0)$ values and τ_D values obtained for these models using the dipole moment fluctuation methodology, as reported in the literature.[3,16−20]

2. METHODS

2.1. Application of an External Electric Field. We consider a system of N particles, atoms, or beads in case a coarse-grained molecular model is used, in a computational box with or without periodic boundary conditions. The interaction between the particles consists of two components: the so-called "bonded interactions" between atoms covalently bound to each other in a molecule and "nonbonded interactions". In a typical biomolecular force field, the bonded interaction terms represent the local interactions between atoms that are separated by one, two, three, or possibly four bonds in a molecule. All other atom pairs interact through nonbonded interactions (generally electrostatic and van der Waals pairwise additive interactions). In addition, the molecular model can be polarizable, i.e., it contains polarizable atoms or sites, leading to a nonpairwise additive electrostatic interaction. When calculating the electrostatic interactions and forces between the particles of a molecule, a given set of particle pairs—the so-called "excluded neighbors" along the covalently bound chain of atoms—is excluded from the nonbonded interaction calculation, because the interaction of the pair, generally determined via quantum chemical or other methods, would be poorly represented as electrostatic, van der Waals, or polarization

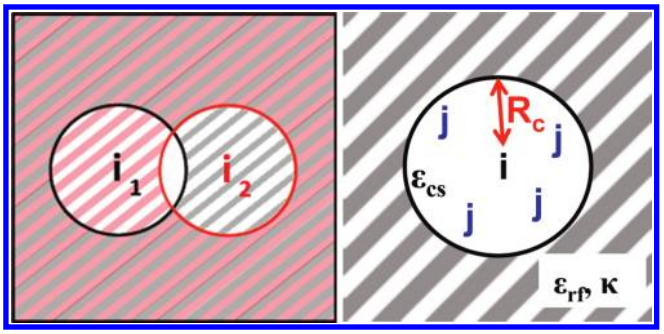

Figure 1. (Left) Schematic picture of the cutoff spheres of two particles i_1 and i_2, and the corresponding overlapping continuum reaction-field regions. (Right) Schematic picture of the interactions between particle i and all particles j in the cutoff sphere with radius $R_c = R_{rf}$.

interactions. The set of particle pairs that is contributing to the nonbonded interaction is additionally limited when a so-called "cutoff sphere" for nonbonded interactions is applied. Since electrostatic interactions are spatially long-ranged, such a cutoff sphere restriction must be supplemented with a continuum or other approximation of the electrostatic interactions for the particle at the center of the cutoff sphere with those beyond it.

We consider an electrostatic nonbonded interaction cutoff sphere with radius R_c around a particle i (see Figure 1). The particles j inside the cutoff sphere have charges q_j, and the static relative dielectric permittivity of the medium inside the cutoff sphere is ε_{cs}. For atomic particles, one generally has $\varepsilon_{cs} = 1$ (i.e., a vacuum background). In a coarse-grained molecular simulation, however, one may have $\varepsilon_{cs} > 1$ (i.e., a dielectric medium that represents the dielectric response of the degrees of freedom that are not considered in the coarse-grained model, via a mean-field response). The dielectric continuum that is intended to represent the electrostatic interactions beyond the cutoff sphere is modeled as a dielectric continuum outside a sphere of radius R_{rf} around particle i, characterized by a relative static permittivity ε_{rf} and an ionic strength I or inverse Debye screening length κ:

$$\kappa^2 = \frac{2IF^2}{\varepsilon_0 \varepsilon_{rf} RT} \tag{1}$$

where F is Faraday's constant, ε_0 the electric permittivity of vacuum, R the gas constant, and T the temperature. Generally, one would choose $R_c = R_{rf}$, but slightly different values for these radii might represent the true interactions better.[7]

The direct Coulomb force on particle i by particle j in the cutoff sphere is

$$\vec{f}_{ij}(r_{ij}) = \frac{q_i q_j}{4\pi\varepsilon_0\varepsilon_{cs}}\left(\frac{\vec{r}_{ij}}{r_{ij}^3}\right) \tag{2}$$

with $\vec{r}_{ij} = \vec{r}_i - \vec{r}_j$. The generalized Poisson−Boltzmann reaction-field force on particle i by particle j can be obtained by solving the Poisson equation inside the cutoff sphere and the Poisson−Boltzmann equation outside it, using the boundary condition of continuous radial dielectric displacement at the boundary $r = R_c = R_{rf}$[15] and zero potential at $r = \infty$,

$$\vec{f}_{ij}(r_{ij}) = -\frac{q_i q_j}{4\pi\varepsilon_0\varepsilon_{cs}}\left(\frac{1}{R_{rf}^3}\right)\left[\frac{(2\varepsilon_{rf}-2\varepsilon_{cs})(1+\kappa R_{rf})+\varepsilon_{rf}(\kappa R_{rf})^2}{(2\varepsilon_{rf}+\varepsilon_{cs})(1+\kappa R_{rf})+\varepsilon_{rf}(\kappa R_{rf})^2}\right]\vec{r}_{ij} \tag{3}$$

The direct Coulomb force on particle i exerted by all particles j in the cutoff sphere, except those that are nearest neighbors and are therefore excluded, is then

$$\vec{f}_i = \sum_{\substack{j \neq i \\ (i,j)\ \text{notexcluded}}}^{N_{cs}} \frac{q_i q_j}{4\pi\varepsilon_0\varepsilon_{cs}}\left(\frac{\vec{r}_{ij}}{r_{ij}^3}\right) \tag{4}$$

and the Poisson−Boltzmann reaction-field force on particle i exerted by all particles j in the cutoff sphere is

$$\vec{f}_i = \frac{q_i}{4\pi\varepsilon_0\varepsilon_{cs}}\left(\frac{1}{R_{rf}^3}\right)\left[\frac{(2\varepsilon_{rf}-2\varepsilon_{cs})(1+\kappa R_{rf})+\varepsilon_{rf}(\kappa R_{rf})^2}{(2\varepsilon_{rf}+\varepsilon_{cs})(1+\kappa R_{rf})+\varepsilon_{rf}(\kappa R_{rf})^2}\right]\sum_{j\neq i}^{N_{cs}} q_j \vec{r}_{ji} \tag{5}$$

where N_{cs} is the number of particles in the cutoff sphere around particle i. Using the short-hand notation,[21]

$$C_{rf} = \frac{(2\varepsilon_{cs}-2\varepsilon_{rf})(1+\kappa R_{rf})-\varepsilon_{rf}(\kappa R_{rf})^2}{(\varepsilon_{cs}+2\varepsilon_{rf})(1+\kappa R_{rf})+\varepsilon_{rf}(\kappa R_{rf})^2} \tag{6}$$

the reaction-field force reads

$$\vec{f}_i = -\frac{q_i}{4\pi\varepsilon_0\varepsilon_{cs}}\left(\frac{C_{rf}}{R_{rf}^3}\right)\vec{M}_i^{cs} = q_i\,\vec{E}_i^{par,rf} \tag{7}$$

where the dipole moment of the cutoff sphere around particle i is denoted by

$$\vec{M}_i^{cs} = \sum_{j\neq i}^{N_{cs}} q_j \vec{r}_{ji} \tag{8}$$

and the corresponding dipolar reaction field in the cutoff sphere induced by the charges of the particles in it is given as

$$\vec{E}_i^{par,rf} = -\frac{1}{4\pi\varepsilon_0\varepsilon_{cs}}\left(\frac{C_{rf}}{R_{rf}^3}\right)\vec{M}_i^{cs} \tag{9}$$

We note that the summation in eq 8 may be extended to include the term for $j = i$, because $\vec{r}_{ii} = 0$.

The potential energy terms corresponding to the forces described by eqs 2 and 3 are, for $i \neq j$,

$$V_{ij}(r_{ij}) = \frac{q_i q_j}{4\pi\varepsilon_0\varepsilon_{cs}}\left\{\frac{1}{r_{ij}} - \left[\frac{(1/2)C_{rf}}{R_{rf}^3}\right]r_{ij}^2 - \frac{1-(1/2)C_{rf}}{R_{rf}}\right\} \tag{10}$$

where the constant term ensures that $V_{ij}(R_{rf}) = 0$. The total electrostatic potential energy of the system then, using the notation $\vec{r}^{\,N} = (\vec{r}_1, \vec{r}_2, ..., \vec{r}_N)$, is given as

$$V(\vec{r}^{\,N}) = \sum_{i=1}^{N-1}\sum_{\substack{j>i \\ j\ \text{inside cut-off}\ i \\ (i,j)\ \text{not excluded}}}^{N} \frac{q_i q_j}{4\pi\varepsilon_0\varepsilon_{cs}}\left(\frac{1}{r_{ij}}\right) - \sum_{i=1}^{N-1}\sum_{\substack{j>i \\ j\ \text{insidecut-off}\ i}}^{N} \frac{q_i q_j}{4\pi\varepsilon_0\varepsilon_{cs}}\left[\frac{(1/2)C_{rf}}{R_{rf}^3}r_{ij}^2 + \frac{1-(1/2)C_{rf}}{R_{rf}}\right] - \sum_{i=1}^{N}\frac{q_i^2}{4\pi\varepsilon_0\varepsilon_{cs}}\left(\frac{1}{2}\right)\left[\frac{1-(1/2)C_{rf}}{R_{rf}}\right] \tag{11}$$

where the third summation is a constant that is added to represent the self-interaction of the charged particles.

If a constant homogeneous external field $\vec{E}^{ext}$ is applied to the system, e.g., along the z-axis,

$$\vec{E}^{ext} = E^{ext}\,\vec{e}_z \tag{12}$$

an additional force on particle i is present,

$$\vec{f}_i^{\,ext,cs} = \frac{q_i}{4\pi\varepsilon_0}\vec{E}^{ext,cs} = \frac{q_i}{4\pi\varepsilon_0}\left(\vec{E}^{ext} + \vec{E}^{ext,rf}\right) \tag{13}$$

where $\vec{E}^{ext,rf}$ describes the contribution to the electric field $\vec{E}^{ext,cs}$ inside the cutoff sphere due to the polarization $\vec{P}^{ext,rf}$ in the dielectric continuum outside the cutoff sphere that is induced by the difference in dielectric permittivity inside the cutoff sphere (ε_{cs}) and outside the cutoff sphere (ε_{rf}). This contribution is dependent on the shape of the cutoff region.[22] For a spherical region, we have

$$\begin{aligned}\vec{E}^{ext,cs} &= \vec{E}^{ext} - \left(\frac{\varepsilon_{cs}-\varepsilon_{rf}}{\varepsilon_{cs}+2\varepsilon_{rf}}\right)\vec{E}^{ext} \\ &= \vec{E}^{ext} + \left(\frac{4\pi}{\varepsilon_{cs}+2\varepsilon_{rf}}\right)\vec{P}^{ext,rf} \\ &= \left(\frac{3\varepsilon_{rf}}{\varepsilon_{cs}+2\varepsilon_{rf}}\right)\vec{E}^{ext}\end{aligned} \tag{14}$$

where the polarization induced around the cutoff cavity in the dielectric continuum by the external field is given as

$$\vec{P}^{ext,rf} = \left(\frac{\varepsilon_{rf}-\varepsilon_{cs}}{4\pi}\right)\vec{E}^{ext} \tag{15}$$

Thus, the electric field in the cutoff sphere has four components:[4] direct and reaction-field components that are due to the particles in the cutoff sphere,

$$\vec{E}_i^{par,cs} = \sum_{\substack{j\neq i \\ \text{exclusions}}}^{N_{cs}} \left(\frac{q_i}{4\pi\varepsilon_0\varepsilon_{cs}}\right)\frac{\vec{r}_{ij}}{r_{ij}^3} \tag{16}$$

$$\vec{E}_i^{par,rf} = -\frac{1}{4\pi\varepsilon_0\varepsilon_{cs}}\left(\frac{C_{rf}}{R_{rf}^3}\right)\vec{M}_i^{cs} \tag{17}$$

the direct external field $\vec{E}^{ext}$ and the reaction field induced by it,

$$\vec{E}^{ext,rf} = -\left(\frac{\varepsilon_{cs}-\varepsilon_{rf}}{\varepsilon_{cs}+2\varepsilon_{rf}}\right)\vec{E}^{ext} \tag{18}$$

The electric field $\vec{E}^{ext}$ that is applied to the system will induce a polarization $\vec{P}$ in the system:[23,24]

$$\vec{P} = \frac{1}{4\pi}(\varepsilon(0)-1)\,\vec{E}^{ext} \tag{19}$$

where $\varepsilon(0)$ is the zero-frequency or static dielectric permittivity of the molecular model. The polarization $\vec{P}$ can be calculated

from the total dipole moment $\vec{M}$ of the system and its volume V:

$$\vec{P} = \frac{\vec{M}}{V} = \frac{1}{V}\sum_{i=1}^{N} q_i \vec{r}_i \quad (20)$$

if $\sum_{i=1}^{N} q_i = 0$. If the latter condition is not satisfied, $\vec{M}$, and, therefore, $\vec{P}$ will be origin-dependent. For a homogeneous external field (see eq 12) along the z-axis, we then find

$$\varepsilon(0) = 1 + 4\pi\frac{\langle M_z\rangle}{VE_z^{ext}} \quad (21)$$

where $\langle M_z\rangle$ is the average dipole moment of the volume V in the z-direction in the simulation.

The method has been implemented into the GROMOS simulation software[25] using the expressions given. However, we note that the electric field eqs 13−21 could also be formulated differently, using

$$\vec{P} = \varepsilon_0(\varepsilon(0) - 1)\,\vec{E}^{ext} \quad (22)$$

instead of eq 19, which would imply

$$\vec{f}_i^{\,ext,cs} = q_i\,\vec{E}^{ext,cs} = q_i(\vec{E}^{ext} + \vec{E}^{ext,rf}) \quad (23)$$

$$\vec{E}^{ext,cs} = \vec{E}^{ext} + \frac{1}{\varepsilon_0}\left(\frac{1}{\varepsilon_{cs} + 2\varepsilon_{rf}}\right)\vec{P}^{ext,rf} \quad (24)$$

$$\vec{P}^{ext,rf} = \varepsilon_0(\varepsilon_{rf} - \varepsilon_{cs})\,\vec{E}^{ext} \quad (25)$$

and

$$\varepsilon(0) = 1 + \left(\frac{1}{\varepsilon_0}\right)\frac{\langle M_z\rangle}{VE_z^{ext}} \quad (26)$$

instead of eqs 13−15 and 21, respectively.

2.2. Calculation of the Dielectric Relaxation Time. The Debye dielectric relaxation time (τ_D) of a molecular liquid can be calculated from an equilibrium MD simulation of the liquid by evaluating the autocorrelation function $\langle\vec{M}(t_0)\cdot\vec{M}(t)\rangle_{t0}$ of the total dipole moment $\vec{M}$ of the system.[26] The averaging is over initial times t_0, i.e., $t \geq t_0$.

It is also possible to obtain a value of τ_D by averaging over a set of nonequilibrium MD simulations that start from a Boltzmann-distributed set of initial configurations and velocities and in which a homogeneous static external electric field $\vec{E}^{ext}$ is switched on at $t = t_0$. This is illustrated in Figure 2. Upon switching on $\vec{E}^{ext}$ along the z-axis at $t = t_0$, the z-component M_z of $\vec{M}$ will increase from its initial value $M_z(t_0)$, the values of which are Gaussian-distributed around $M_z = 0$, to a steady-state value $M_z(t = \infty)$. For a Debye dielectric medium, this buildup will be exponential:

$$\langle M_z(t)\rangle_{t_0} = \langle M_z(t = \infty)\rangle_{t_0}\left[1 - \exp\left(-\frac{t - t_0}{\tau_M}\right)\right] \quad (27)$$

The value of $\langle M_z(t = \infty)\rangle_{t0}$ will be larger for larger E_z^{ext}, but different field strengths E_z^{ext} should yield the same τ_M, as long as E_z^{ext} is not too small and not too large. The relationship between τ_M and τ_D is given as

$$\tau_D = \left[\frac{\varepsilon(0) + 2 + C_{rf}(\varepsilon(0) - 1)}{3}\right]\tau_M \quad (28)$$

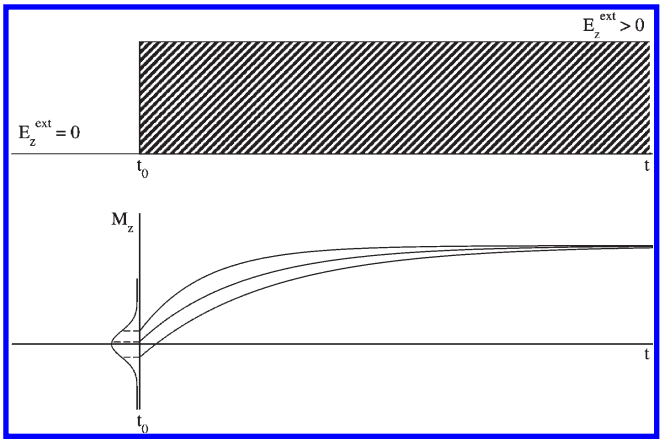

Figure 2. Sketch of the relaxation of the total dipole moment $M_z(t)$, as a function of time upon switching on a homogeneous static electric field E_z^{ext} at time t_0, for three different nonequilibrium molecular dynamics (MD) simulations.

which is a generalization for $\kappa \geq 0$ of the relationship for $\kappa = 0$ given by Neumann.[27] The value of $\varepsilon(0)$ can be calculated using eq 21, in which $\langle M_z\rangle = \langle M_z(t = \infty)\rangle_{t0}$.

2.3. Simulation Details. The molecular models for water (H_2O), dimethylsulfoxide (DMSO), methanol (MeOH), and chloroform ($CHCl_3$) that have been chosen to test the external field methodology were the models for which the dielectric properties calculated with the dipole-fluctuation method had been reported in the literature.[16−20] The geometry of these rigid models was maintained using the SHAKE algorithm,[28] with a relative accuracy of 10^{-4}. All simulations were performed under NpT conditions using a modified version of the GROMOS05 package of programs.[25] The temperature was kept to a reference value by weak coupling to a temperature bath with a relaxation time of 0.1 ps,[6] and the pressure was maintained at 1.013 bar (1 atm) using the same type of algorithm, with a relaxation time of 0.5 ps and the experimental isothermal compressibility of the corresponding solvent. The integration time step was 2 fs. For the nonbonded interactions, a twin-range method was used with cutoff radii of 0.8 nm (short-range) and 1.4 nm (long-range). Outside the long-range cutoff, a reaction-field correction[15] with a relative dielectric permittivity (ε_{rf}) of 78.5[20] for SPC water, 46[18] for DMSO, 32.63[17] for methanol, and 5[16] for chloroform was applied. Values of $\varepsilon_{cs} = 1$, $\kappa = 0$, and $R_{rf} = 1.4$ nm were used. The pair list for pairs within the short-range cutoff and the energies and forces for long-range pairs were updated every 10 fs (5 steps). Cubic boxes of 5384 SPC water molecules (initial box length = 5.49 nm), 429 DMSO molecules (initial box length = 3.69 nm), 661 methanol molecules (initial box length = 3.60 nm), and 1000 chloroform molecules (initial box length = 5.11 nm) were used, together with periodic boundary conditions. To calculate $\varepsilon(0)$ for each electric field strength, an equilibration simulation of 100 ps and, subsequently, a 500 ps production run was performed at 298 K. The box dipole moment and the volume were saved every 0.4 ps (200 steps), and the atom positions every 2.0 ps (1000 steps) for analysis. The values of τ_D were obtained from 100 short (30 ps) nonequilibrium simulations at two different electric field strengths. The box dipole moment and the volume were saved every step for analysis. The 100 starting configurations were taken from an equilibrium simulation of 1-ns length, where the configuration was saved every 10 ps. The two

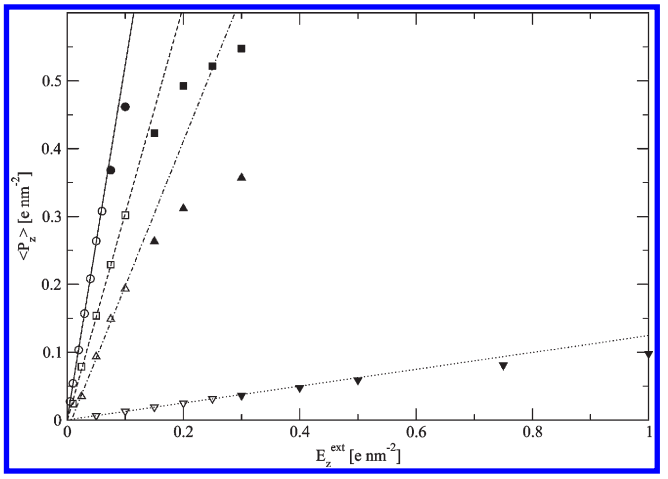

Figure 3. Dependence of the polarization averaged over time $\langle P_z \rangle$ on the applied electric field E_z^{ext} for different solvents: H_2O (circles), DMSO (squares), MeOH (triangles), and $CHCl_3$ (inverted triangles). Lines represent results obtained from linear regression: (—) H_2O, (- - -) DMSO, (- · -) MeOH, and (· · ·) $CHCl_3$. When $\mu_i E_z^{ext}/(3k_B) > 50$ K,[29,30] where μ is the molecular dipole moment, the data (full symbols) were excluded from linear regression.

electric field strengths were chosen for each solvent, such that they are as large as possible while being in the linear-response regime. With regard to DMSO, no value for τ_D obtained from the time correlation function of the dipole moment in an equilibrium simulation was reported in the literature, it was therefore calculated from a 1-ns equilibrium simulation, where the configurations were saved every 0.2 ps (100 steps) for analysis.

3. RESULTS

3.1. Static Dielectric Permittivity $\varepsilon(0)$. In short simulations for the models of four different molecular liquids (H_2O, DMSO, MeOH, and $CHCl_3$), an external electric field of varying strength was applied in the z-direction and the resulting polarization of the box was measured. In Figure 3, the polarization in z-direction is shown as a function of the strength of the applied field. For small fields, the energy of the molecular dipole μ in the field is much smaller than k_BT, i.e., $\mu_i E_z^{ext}/3k_B \ll T$,[29] the response of $\vec{P}$ to $\vec{E}^{ext}$ is linear and only these data points (open symbols) were considered in the calculation of the dielectric permittivity $\varepsilon(0)$. For high field strengths, the relationship becomes nonlinear because of saturation effects (full symbols). The slope of the fitted linear function was used in eq 21, and the resulting $\varepsilon(0)$ values are shown in Table 1, together with the experimental values and those obtained using the dipole moment fluctuation methodology, as reported in the literature. For H_2O, DMSO, and $CHCl_3$, the values for $\varepsilon(0)$ resulting from the external field method agree well with values from the fluctuation method. For MeOH, the values differ, which could be due to the factors used to set up the various simulations: size of the system, constant volume versus constant pressure condition, cutoff radii and update frequency of the nonbonded interaction pairlist, equilibration and simulation time periods. Since the dielectric permittivity is a global property of the system, it converges slowly, especially for high values. We note that all simulations from which the dielectric permittivity was calculated, using the dipole moment fluctuation method,[16−18,20] were of rather short length. To obtain well-converged values with this method, simulations

Table 1. Experimental and Calculated Values for the Relative Static Dielectric Permittivity $\varepsilon(0)$ at 298 K and 1 atm for Water (H_2O), Dimethylsulfoxide (DMSO), Methanol (MeOH), and Chloroform ($CHCl_3$)[a]

	$\varepsilon(0)$		
solvent	expt	fluctuation formula	applied field method
H_2O	78.5[31]	66.6[20]	66.7
DMSO	46[32]	38[18]	39.5
MeOH	32.63[31]	19.8[17]	27.8
$CHCl_3$	4.81[31]	2.4[16]	2.6

[a] The lengths of the simulations for which the dipole moment fluctuation methodology was used were 3 ns,[20] 2 ns,[18] 2 ns,[17] and 1.2 ns.[16]

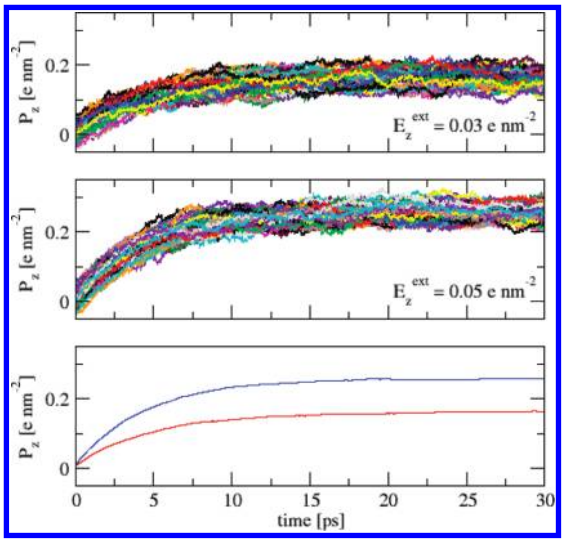

Figure 4. Polarization $P_z(t)$ for 100 nonequilibrium MD simulations of liquid water (5384 SPC molecules) after switching on an electric field E_z^{ext} at $t_0 = 0$, for $E_z^{ext} = 0.03\ e\ \mathrm{nm}^{-2}$ (upper panel) and $E_z^{ext} = 0.05\ e\ \mathrm{nm}^{-2}$ (middle panel). The averages over the 100 trajectories are shown in red ($E_z^{ext} = 0.03\ e\ \mathrm{nm}^{-2}$) and blue ($E_z^{ext} = 0.05\ e\ \mathrm{nm}^{-2}$) in the lower panel.

of periods of many nanoseconds should be performed, while 500 ps per field strength E^{ext} are sufficient using an applied external field. A 10-ns equilibrium simulation of the MeOH system, i.e., $E^{ext} = 0$, was analyzed using the dipole moment fluctuation formula and gave $\varepsilon(0) = 24.4$.

3.2. Debye Dielectric Relaxation Time (τ_D). In Figure 4, the relaxation of $P_z(t)$ and $\langle P_z(t) \rangle_{t0}$ toward $\langle P_z(t = \infty) \rangle_{t0}$ for liquid water is shown for two different electric field strengths. With increasing field strength, $\langle P_z(t = \infty) \rangle_{t0}$ increases and its variation decreases. However, both field strengths yield similar τ_D values, which are close to those obtained using the equilibrium time correlation function of $\vec{M}$, as reported in the literature. The values of τ_D derived from the relaxation for all four test solvents are given in Table 2. The value obtained using the fluctuation formula, $\tau_D = 12.3$ ps, is not very precise, because of the short length of 1 ns of this simulation.

4. DISCUSSION

The models that were used for H_2O, DMSO, MeOH, and $CHCl_3$ were rigid (i.e., they did not possess internal degrees of

Table 2. Experimental and Calculated Values for the Debye Dielectric Relaxation Time τ_D at 298 K and 1 atm for Water (H_2O), Dimethylsulfoxide (DMSO), Methanol (MeOH), and Chloroform ($CHCl_3$)[a]

	τ_D[ps]		Applied Field Method			
solvent	expt	fluctuation formula	E_z^{ext} [e nm^{-2}]	τ_D [ps]	E_z^{ext} [e nm^{-2}]	τ_D [ps]
H_2O	8.3[33]	6.2[20]	0.03	6.6	0.05	6.0
DMSO	18.5[34]	12.3	0.05	9.6	0.075	9.7
MeOH	49[35]	14[17]	0.075	14.7	0.1	14.1
$CHCl_3$	5.4[36]	3.8[16]	0.2	4.2	0.4	4.3

[a] The electric field strengths were chosen such that they were as large as possible while within the linear-response regime.

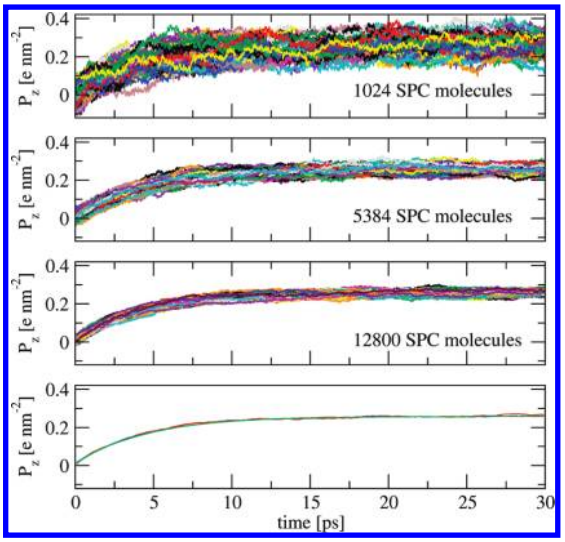

Figure 5. Polarization $P_z(t)$ for 100 nonequilibrium MD simulations of liquid water using three different system sizes (1024, 5384, and 12800 SPC molecules), after switching on an electric field $E_z^{ext} = 0.05\ e\ \mathrm{nm}^{-2}$ at $t_0 = 0$. The averages over the 100 trajectories are shown in red (1024 molecules), blue (5384 molecules), and green (12800 molecules) in the lowest panel.

freedom). This meant that no vibrational contributions of such degrees of freedom to $\varepsilon(0)$ or τ_D were present.

Recently, the correlations in the total dipole moment $\vec{M}$ of a Stockmayer liquid were analyzed in equilibrium MD simulations using periodic boundary conditions and either a lattice-sum (Ewald) or a reaction-field method to approximate the long-range electrostatic interactions.[37] For the strongly polar Stockmayer model used, the fluctuations of $\vec{M}$ were observed to be dependent on the relative size of the cutoff sphere and the computational periodic box. In other words, a dependence of $\langle \vec{M}^2 \rangle$ on the system size was reported. Therefore, we investigated the system size dependence of the values of $\varepsilon(0)$ and τ_D obtained with the external field method, using liquid water as the test system. The results are shown in Figure 5 and Table 3. While the variation of $P_z(t = \infty)$ decreases as the system size increases, because of better statistics, the average relaxation is independent of the system size (lowest panel in Figure 5), and so are the values obtained for τ_D and $\varepsilon(0)$.

One could think of avoiding periodicity artifacts by using a fixed nonperiodic spherical boundary in combination with the image charge representation of the reaction field.[38] However, such an approach introduces wall effects, which cannot easily be compensated via the use of special wall forces.[39−41]

Table 3. Calculated Values for the Relative Static Dielectric Permittivity $\varepsilon(0)$ and the Debye Dielectric Relaxation Time τ_D at 298 K and 1 atm for Water Using Three Different System Sizes and Two Different Electric Field Strengths[a]

number of H_2O	$\varepsilon(0)$	E_z^{ext}[e nm^{-2}]	τ_D[ps]	E_z^{ext}[e nm^{-2}]	τ_D[ps]
1024	63	0.03	6.1	0.05	6.0
5384	67	0.03	6.6	0.05	6.0
12 800	64	0.03	6.3	0.05	6.0

[a] The electric field strengths were chosen such that they were as large as possible while within the linear-response regime.

5. SUMMARY AND CONCLUSIONS

Expressions for the calculation of the static relative dielectric permittivity ($\varepsilon(0)$) and the Debye dielectric relaxation time (τ_D) of a molecular model from MD simulations of the liquid phase, where a constant external electric field is applied, were given for the case in which a spherical truncation with $\varepsilon_{cs} \geq 1$ inside the cutoff sphere combined with a Poisson−Boltzmann continuum reaction-field with $\kappa \geq 0$ outside the cutoff sphere is used. The external field method was applied to molecular models of four different molecular liquids (water (H_2O), dimethylsulfoxide (DMSO), methanol (MeOH), and chloroform ($CHCl_3$)), and the results were compared to values obtained through the dipole moment fluctuation methodology and from experiment. The dielectric permittivities and relaxation times calculated using the external field method agree with values resulting from the fluctuation method. The external field method is simple to implement and, compared to the dipole moment fluctuation methodology, it is computationally more efficient and can also be applied to uncharged, but polarizable molecular models or in coarse-grained simulations, where $\varepsilon_{cs} > 1$ is used.

AUTHOR INFORMATION

Corresponding Author

*E-mail: wfvgn@igc.phys.chem.ethz.ch.

ACKNOWLEDGMENT

We thank Phillippe Hünenberger for useful discussion. The financial support by the National Center of Competence in Research (NCCR) in Structural Biology, the Swiss National Science Foundation (Grant No. 200020-121913), and the European Research Council (Grant No. 228076) is gratefully acknowledged.

REFERENCES

(1) Allen, M. P.; Tildesley, D. J. *Computer Simulation of Liquids*; Clarendon Press: Oxford, U.K., 1987.
(2) Neumann, M. *Mol. Phys.* **1983**, *50*, 841.
(3) Heinz, T. N.; van Gunsteren, W. F.; Hünenberger, P. H. *J. Chem. Phys.* **2001**, *115*, 1125.
(4) Adams, D. J.; Adams, E. M. *Mol. Phys.* **1981**, *42*, 907.
(5) Berendsen, H. J. C. Transport Properties Computed by Linear Response through Weak Coupling to a Bath. In *Computer Simulation in Materials Science*; Meyer, M., Pontikis, V., Eds.; Kluwer Academic Publishers: Dordrecht, The Netherlands, 1991; pp 139−155.

(6) Berendsen, H. J. C.; Postma, J. P. M.; van Gunsteren, W. F.; DiNola, A.; Haak, J. R. *J. Chem. Phys.* **1984**, *81*, 1517.
(7) Luty, B. A.; van Gunsteren, W. F. *J. Phys. Chem.* **1996**, *100*, 2581.
(8) Hünenberger, P. H.; McCammon, J. A. *J. Chem. Phys.* **1999**, *110*, 1856.
(9) Hünenberger, P. H.; McCammon, J. A. *Biophys. Chem.* **1999**, *78*, 69.
(10) Weber, W.; Hünenberger, P. H.; McCammon, J. A. *J. Phys. Chem. B* **2000**, *104*, 3668.
(11) Nymand, T. M.; Linse, P. *J. Chem. Phys.* **2000**, *112*, 6386.
(12) Walser, R.; Hünenberger, P. H.; van Gunsteren, W. F. *Proteins* **2001**, *43*, 509.
(13) Tironi, I. G; Luty, B. A.; van Gunsteren, W. F. *J. Chem. Phys.* **1997**, *106*, 6068.
(14) Barker, J. A.; Watts, R. O. *Mol. Phys.* **1973**, *26*, 789.
(15) Tironi, I. G.; Sperb, R.; Smith, P. E.; van Gunsteren, W. F. *J. Chem. Phys.* **1995**, *102*, 5451.
(16) Tironi, I. G.; van Gunsteren, W. F. *Mol. Phys.* **1994**, *83*, 381.
(17) Walser, R.; Mark, A. E.; van Gunsteren, W. F. *J. Chem. Phys.* **2000**, *112*, 10450.
(18) Geerke, D. P.; Oostenbrink, C.; van der Vegt, N. F. A.; van Gunsteren, W. F. *J. Phys. Chem. B* **2004**, *108*, 1436.
(19) Smith, P. E.; van Gunsteren, W. F. *J. Chem. Phys.* **1994**, *100*, 3169.
(20) Glättli, A.; Daura, X.; van Gunsteren, W. F. *J. Chem. Phys.* **2002**, *116*, 9811.
(21) van Gunsteren, W. F.; Billeter, S. R.; Eising, A. A.; Hünenberger, P. H.; Krüger, P.; Mark, A. E.; Scott, W. R. P.; Tironi, I. G. *Biomolecular Simulation: The GROMOS96 Manual and User Guide*; vdf Hochschulverlag AG an der ETH Zürich: Zürich, Switzerland, 1996.
(22) Panofsky, W. K. H.; Phillips, M. *Classical Electricity and Magnetism*, 2nd ed.; Addison−Wesley: Reading, MA, 1964.
(23) Böttcher, C. J. F. *Dielectrics in Static Fields*; Theory of Electric Polarization, Vol. 1; Elsevier Science Publishers: Amsterdam, The Netherlands, 1973.
(24) Böttcher, C. J. F.; Bordewijk, P. *Dielectrics in Time-Dependent Fields*; Theory of Electric Polarization, Vol. 2; Elsevier Science Publishers: Amsterdam, The Netherlands, 1978.
(25) Christen, M.; Hünenberger, P. H.; Bakowies, D.; Baron, R.; Bürgi, R.; Geerke, D. P.; Heinz, T. N.; Kastenholz, M. A.; Kräutler, V.; Oostenbrink, C.; Peter, C.; Trzesniak, D.; van Gunsteren, W. F. *J. Comput. Chem.* **2005**, *26*, 1719.
(26) Neumann, M.; Steinhauser, O. *Chem. Phys. Lett.* **1983**, *102*, 508.
(27) Neumann, M. *J. Chem. Phys.* **1985**, *82*, 5663.
(28) Ryckaert, J.-P.; Ciccotti, G.; Berendsen, H. J. C. *J. Comput. Phys.* **1977**, *23*, 327.
(29) Evans, W. A. B.; Powles, J. G. *Mol. Phys.* **1982**, *45*, 695.
(30) Kunz, A. P. E.; Eichenberger, A. P.; van Gunsteren, W. F. *Mol. Phys.* **2010**, *109*, 365.
(31) Lide, D. R. *Handbook of Chemistry and Physics*, 88th ed.; CRC Press/Taylor and Francis: Boca Raton, FL, 2007−2008.
(32) Riddick, J. A.; Bunger, W. B.; Sakand, T. K. *Organic Solvents: Physical Properties and Methods of Purification*; John Wiley and Sons: New York, 1986.
(33) Kaatze, U. *J. Chem. Eng. Data* **1989**, *34*, 371.
(34) Kaatze, U.; Pottel, R.; Schaefer, M. *J. Phys. Chem.* **1989**, *93*, 5623.
(35) Barbenza, G. H. *J. Chim. Phys. Phys.−Chim. Biol.* **1968**, *65*, 906.
(36) Antony, A. A.; Smyth, C. P. *J. Am. Chem. Soc.* **1964**, *86*, 152.
(37) Stenhammar, J.; Linse, P.; Karlström, G. *J. Chem. Phys.* **2009**, *131*, 164507.
(38) Friedman, H. L. *Mol. Phys.* **1975**, *29*, 1533.
(39) Juffer, A. H.; Botta, E. F. F.; van Keulen, B. A. M.; van der Ploeg, A.; Berendsen, H. J. C. *J. Comput. Phys.* **1991**, *97*, 144.
(40) Juffer, A. H.; Berendsen, H. J. C. *Mol. Phys.* **1993**, *79*, 623.
(41) Juffer, A. H. *On the Modelling of Solvent Mean Force Potentials*, Ph.D. Thesis, University of Groningen, The Netherlands, 1993.